

Optical absorption by excitons in semiconductor quantum wells in tilted magnetic and electric fields

B. S. Monozon* and P. Schmelcher

Zentrum für Optische Quantentechnologien, Universität Hamburg, Luruper Chaussee 149, D-22761 Hamburg, Germany

(Received 17 July 2010; revised manuscript received 23 September 2010; published 10 November 2010)

An analytical approach to the problem of the fundamental and exciton magnetoelectroabsorption in a narrow quantum well (QW) is developed. The external magnetic and electric fields are parallel and both tilted with respect to the QW growth axis. The width of the QW is taken to be much less than the magnetic length and the exciton Bohr radius. The effect of the electric field on size quantized states reduces to the size-quantized Stark shift of the well subbands. Analytical dependencies of the coefficient of the optical absorption and the exciton binding energy on the strengths of the external fields, width of the QW, exciton parameters and tilt angle are obtained and discussed. Novel effects forbidden in bulk material are found to occur. These are based on the interplay between the parallel magnetic and electric fields which in turn is caused by the splitting of the tilted fields into transverse and longitudinal components. In particular, an inversion effect is revealed. Estimates of the expected experimental values are provided for GaAs/AlGaAs QW.

DOI: [10.1103/PhysRevB.82.205313](https://doi.org/10.1103/PhysRevB.82.205313)

PACS number(s): 73.21.Fg, 71.35.Cc

I. INTRODUCTION

The pioneering works of Maan¹ and Merlin² and the rapid advance in material growth technology lead to a renewed interest in theoretical and experimental studies of semiconductor QWs subject to tilted magnetic fields \vec{B} directed at an angle ϑ with respect to the QW axis. In such structures investigations of cyclotron resonance, spin-flip transitions, crossing and anticrossing of spin-split Landau levels, as well as transport properties are under way (see Ref. 3 and references therein). The reason for this interest is the fact that QWs represent unique structures providing us with novel electronic,^{1,2} optical,⁴ and transport⁵ effects. In the case of tilted fields these phenomena are based on the breaking of the cylindrical symmetry caused by the effective decomposition of the magnetic field \vec{B} into two components: the longitudinal \vec{B}_{\parallel} directed parallel to the QW axis and transverse \vec{B}_{\perp} which lies in the heteroplane. An electric field \vec{F} directed parallel to the magnetic field additionally enriches the observed physical properties. In bulk material parallel external magnetic and electric fields do not interfere in terms of their action on the electron states: the magnetic field acts on the transverse motion while the electric field governs the longitudinal motion. This does not hold in case of a QW. The well potential suppresses the effects of the \vec{F}_{\parallel} and \vec{B}_{\perp} components. As a result the electron states are predominantly affected by the influence of the interfering crossed \vec{B}_{\parallel} and \vec{F}_{\perp} fields.

Investigations of excitons in the above setup are of particular relevance since their optical properties change drastically in QWs. In particular Rydberg series of exciton peaks arise below the edge, determined by the electron-hole size-quantized energy levels. In the presence of an electric field F the exciton peaks become wider and less in intensity due to the ionization of the bound exciton states. Under the condition $F > F_c$, where $F_c \approx E_b/ea_0$ is the critical electric field, linked with the exciton binding energy E_b and the exciton Bohr radius a_0 , exciton ionization is an important process. This is why narrow QWs of width d , which is much smaller

than the exciton Bohr radius a_0 ($d \ll a_0$) are of particular interest. While in the units of the exciton Rydberg constant Ry the binding energy of the exciton in bulk material is $E_b^{(3D)} = 1Ry$, the two-dimensional (2D) exciton in such a QW possesses the binding energy $E_b^{(2D)} = 4Ry$. Also the oscillator strengths of the ground peaks of the exciton optical absorption are $f^{(3D)} \sim a_0^{-3}$ compared to $f^{(2D)} \sim 8a_0^{-2}$. We therefore encounter an increase in both the stability of the 2D exciton states and the intensities of the corresponding exciton peaks.

In contrast to the problem of confined excitons in the presence of tilted magnetic fields, or electric fields, which have been explored by many authors, low dimensional excitons simultaneously exposed to both fields have received little attention. During the last decade indirect excitons in a double QW in the presence of magnetic and electric fields have been considered in a few works. Butov *et al.*⁶ and Dios-Leyva *et al.*⁷ studied the case where the magnetic field is directed parallel and perpendicular to the growth axis, respectively, while Morales *et al.*⁸ used in-plane magnetic fields. In these works the electric field was chosen to be parallel to the growth axis. Impurities⁹ and excitons¹⁰ in quantum dots (QDs) have been considered for the electric field parallel to the growth axis and for both longitudinal and transverse magnetic fields. Recently effects of an arbitrary tilted electric field on the magnetoexciton in a cylindrical QD have been studied in Ref. 11 for the magnetic field parallel to the QD axis.

A study of excitons in a narrow QW in the presence of tilted parallel magnetic and electric fields is important on account of three aspects: (i) excitons are present in the absolute majority of semiconductors and represent an integral part of them, (ii) the effective splitting of the combined fields caused by the QW potential, provides an additional handle on excitonic properties, and (iii) a wide range of potential applications of this setup occur in, e.g., infrared detectors, modulators, and lasers. Note that in particular a narrow QW provides an enhancement of both the excitonic effects and the effective decomposition of the external fields into different components.

Two comments are in order. First, the theoretical methods employed so far in the literature are mostly based on numerical, mostly variational, approaches requiring substantial computational efforts. In spite of this a detailed evaluation of the optical absorption spectrum depending on the width of the QW, strengths of the magnetic and electric fields, and especially of the tilt parameter are not available. Numerical approaches are indispensable for a detailed comparison with the experimental data. However the analytical method applied and/or developed in the present work are complementary in the sense that they provide the possibility to follow the evolution of the exciton states as a function of the parameters of the QW and the external fields. Second, electronic and excitonic states in a single QW subject to parallel but arbitrarily tilted magnetic and electric fields have not been theoretically investigated. Note, that a parallel orientation of the fields allows to demonstrate the effects due to splitting of these fields into longitudinal and transverse components and subsequent interaction effects which are not present in bulk material.

We develop an analytical approach to the problem of exciton magnetoelectroabsorption in a narrow QW in the presence of parallel external magnetic and electric fields both arbitrarily directed with respect to the QW axis. The width of the QW is taken to be much less than the magnetic length and the exciton Bohr radius. The effective mass approximation for the ellipsoidal electron and hole energy bands is employed. Analytical dependencies of the coefficient of the optical absorption and the exciton binding energy on the strengths of the external fields, width of the QW, exciton parameters and tilt angle are obtained and discussed. We take into account the center of mass electric field $F_{\text{cm}} = \hbar B_{\parallel} K_{\perp} / M$ (Ref. 12) acting on the relative motion of the exciton of total mass M , involving the in-plane component of the pseudomomentum K_{\perp} . Novel effects based on the interplay between the parallel magnetic and electric fields, which is absent in bulk material, are found to occur. In particular the interplay between the F_{cm} and external F_{\perp} electric fields induces the inversion effect, i.e., the change in the exciton states while reversing the orientation of the parallel magnetic \vec{B} or electric \vec{F} fields or \vec{K}_{\perp} . Estimates of the expected experimental values are given for the parameters of a GaAs/AlGaAs QW and it is shown that the above-mentioned effects can be observed experimentally. Our analytical results are qualitatively and also quantitatively in line with those obtained numerically. We note, that our aim is to elucidate the basic physics of the excitonic behavior by deriving closed form analytical expressions thereby motivating further experiments. We do not intend to compete with the results obtained by comprehensive numerical methods.

The paper is organized as follows. In Sec. II the general analytical approach to the calculation of the coefficient of the optical magnetoelectroabsorption in a narrow QW subject to tilted external fields is developed. The spectrum of the exciton absorption is given in Sec. III in an explicit form. A discussion of the obtained results and estimates of the expected experimental values relevant to GaAs/AlGaAs QWs and typical strengths of the magnetic and electric fields are provided in Sec. IV. Section V contains the conclusions.

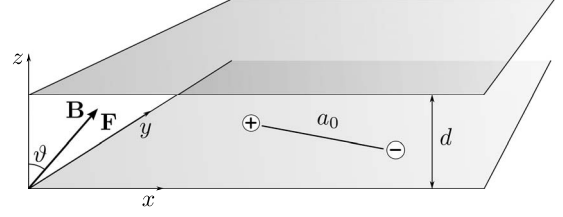


FIG. 1. Schematic illustration of the setup. Exciton Bohr radius a_0 in the QW of width d in magnetic \vec{B} and electric \vec{F} fields directed at an angle ϑ with respect to the QW z axis.

II. GENERAL THEORY

We consider an exciton formed by a spinless electron (e) and hole (h) both in parabolic, nondegenerate energy bands described by the longitudinal (\parallel) and transverse (\perp) effective masses $m_{\parallel,\perp j}$ ($j=e,h$) respectively and separated by a wide energy gap E_g . The parallel magnetic \vec{B} and electric \vec{F} fields are directed at an angle ϑ to the QW growth z axis. The QW is treated as a square well of width d bounded by the infinite barriers at the heteroplanes $z = \pm d/2$ (see Fig. 1 for details). The parameters relevant to the calculation are the exciton Bohr radius $a_{0\parallel,\perp}$ and the magnetic length $a_{B\parallel,\perp}$

$$a_{0\parallel,\perp} = \frac{4\pi\epsilon_0\epsilon\hbar^2}{\mu_{\parallel,\perp}e^2}; \quad a_{B\parallel,\perp} = \sqrt{\frac{\hbar}{eB_{\parallel,\perp}}},$$

where ϵ is the dielectric constant, $\mu_{\parallel,\perp}^{-1} = m_{\text{ell},\perp}^{-1} + m_{h\parallel,\perp}^{-1}$ is the reciprocal reduced effective mass, and $a_{\parallel} = a \cos \vartheta$, $a_{\perp} = a \sin \vartheta$ are the longitudinal and transverse components of a vector $\vec{a} = \vec{a}_{\perp} + a_{\parallel}\vec{e}_z$ ($\vec{r} = \vec{\rho} + z\vec{e}_z$). The parameters

$$y_0 = \frac{M_{\perp}\tilde{F}_{\perp}}{eB_{\parallel}^2}; \quad \left(s_0 = \frac{y_0^2}{2a_{B\parallel}^2} \right)$$

describe the shift of the trajectory induced by the electric field \tilde{F}_{\perp} directed perpendicular to the magnetic field B_{\parallel} .

In the effective mass approximation the equation describing the exciton in the QW in the presence of parallel tilted magnetic $\vec{B} = \vec{\nabla} \times \vec{A}$ (\vec{A} is the vector potential) and electric \vec{F} fields has the form

$$\left\{ \sum_{j=e,h} \left[\frac{1}{2m_{\perp j}} (-i\hbar\vec{\nabla}_{\perp j} + e_j\vec{A}_{\perp j})^2 + \frac{1}{2m_{\parallel j}} \left(-i\hbar\frac{\partial}{\partial z_j} + e_jA_{zj} \right)^2 - e_j\vec{F}\vec{r}_j \right] - \frac{e^2}{4\pi\epsilon_0\epsilon|\vec{r}_e - \vec{r}_h|} \right\} \Psi(\vec{r}_e, \vec{r}_h) = E\Psi(\vec{r}_e, \vec{r}_h);$$

$$e_e = -e_h = e. \quad (1)$$

By solving this equation subject to the boundary conditions

$$\Psi\left(\vec{\rho}_e, \pm \frac{d}{2}; \vec{\rho}_h, \pm \frac{d}{2}\right) = 0 \quad (2)$$

the exciton energy E and the wave function Ψ can be found, in principle.

For the $\vec{e}_z, \vec{F}, \vec{B}, \vec{e}_y$ planar geometry we take $A_x = -(1/2)B_{\parallel}y$; $A_y = (1/2)B_{\parallel}x$, $A_z = -B_{\perp}x$ and then substitute the function

$$\Psi(\vec{r}_e, \vec{r}_h) = \exp\left\{i\frac{eB_{\perp}}{\hbar}(x_e z_e - x_h z_h)\right\} G(\vec{r}_e, \vec{r}_h) \quad (3)$$

into Eq. (1). The function G obeys the equation

$$\left\{ \sum_{j=e,h} \left(\frac{1}{2m_{\perp j}} \left[\left(-i\hbar\vec{\nabla}_{\perp j} - \frac{1}{2}e_j[\vec{B}_{\parallel} \times \vec{\rho}_j] \right)^2 - 2i\hbar e_j B_{\perp} z_j \frac{\partial}{\partial x_j} - e^2 B_{\parallel} B_{\perp} z_j y_j + e^2 B_{\perp}^2 z_j^2 \right] - \frac{\hbar^2}{2m_{\parallel j}} \frac{\partial^2}{\partial z_j^2} - e_j F_{\perp} y_j - e_j F_{\parallel} z_j \right) - \frac{e^2}{4\pi\epsilon_0\epsilon|\vec{r}_e - \vec{r}_h|} \right\} G(\vec{r}_e, \vec{r}_h) = EG(\vec{r}_e, \vec{r}_h). \quad (4)$$

Below we consider a narrow QW in which the longitudinal motion parallel to the QW z axis is governed by the well potential slightly perturbed by the transverse magnetic B_{\perp} and longitudinal electric F_{\parallel} fields and the Coulomb field of the exciton $\sim -|\vec{r}_e - \vec{r}_h|^{-1}$. In this case the energies of the size quantization $\sim d^{-2}$ are much larger than the distance between the neighboring Landau levels $\sim a_{B_{\perp}}^{-2}$ and the energies acquired by the carriers in the presence of the electric field F_{\parallel} at distance d . This implies the conditions

$$d \ll a_{B_{\perp}}, a_{0\parallel}; \quad d^3 \ll \frac{\hbar^2 \pi^2}{\mu_{\parallel} e F_{\parallel}}. \quad (5)$$

In the adiabatic approximation justified by the condition (5) the wave function G reads

$$G_{n_e, n_h}(\vec{r}_e, \vec{r}_h) = f_{n_e}(z_e) f_{n_h}(z_h) \Phi_{n_e, n_h}(\vec{\rho}_e, \vec{\rho}_h), \quad (6)$$

where

$$f_{n_j}(z_j) = \sqrt{\frac{2}{d}} \sin\left(\frac{z_j}{d} + \frac{1}{2}\right) n_j \pi; \quad n_j = 1, 2, \dots; \quad j = e, h \quad (7)$$

are the wave functions of the carriers in the QW.

Compared to the 2D Coulomb field the longitudinal magnetic field B_{\parallel} will be considered as weak ($a_{0\perp}/a_{B_{\parallel}} \ll 1$) or strong ($a_{0\perp}/a_{B_{\parallel}} \gg 1$) while the transverse electric field F_{\perp} remains to be weak ($F_{\perp} \ll e/4\pi\epsilon_0\epsilon a_{0\perp}^2$). However, relatively to the magnetic field B_{\parallel} the same electric field F_{\perp} will be defined as weak ($s_0 \ll 1$) or strong ($s_0 \gg 1$) [see Eq. (14) for the explicit form of s_0]. The nonrelativistic approach implies the smallness of the drift velocity of the carriers $v_D = F_{\perp}/B_{\parallel}$ relatively to the speed of light c , that in turn imposes on the strengths of the fields B , F and on the tilted angle ϑ the condition $F \tan \vartheta / Bc \ll 1$, realized practically for all regions of the fields and angles typically employed in experiment.

In Eq. (4) the terms $\sim B_{\perp}^2 z_j^2$ and $\sim B_{\perp} z_j$, $B_{\perp} B_{\parallel} z_j$, $F_{\parallel} z_j$ contribute to the size-quantized energy levels in first and second order of perturbation theory, respectively. The contribution of the magnetic field-dependent linear terms $\sim z_j$ compared to the square term $\sim B_{\perp}^2 z_j^2$ is of the order $(d/a_{B_{\parallel}})^2$ for strong magnetic fields ($a_{B_{\parallel}} \ll a_{0\perp}$) and of order

$(d/a_{B_{\parallel}})^2 (a_{0\perp}/a_{B_{\parallel}})^2$ for weak magnetic fields ($a_{B_{\parallel}} \gg a_{0\perp}$). We ignore the contribution of the linear terms due to the validity of $d \ll a_{B_{\parallel}}$.

We introduce the transverse coordinates of the center of mass \vec{R}_{\perp} and the relative coordinate $\vec{\rho}$ defined as usual by

$$\vec{R}_{\perp} = \frac{m_{\perp e} \vec{\rho}_e + m_{\perp h} \vec{\rho}_h}{M_{\perp}}; \quad M_{\perp} = m_{\perp e} + m_{\perp h}; \quad \vec{\rho} = \vec{\rho}_e - \vec{\rho}_h.$$

Substituting the function (6) into Eq. (4) with

$$\Phi_{n_e, n_h}(\vec{\rho}_e, \vec{\rho}_h) = \frac{1}{\sqrt{S}} \exp\left\{i\left(\vec{K}_{\perp} + \frac{e}{2\hbar}[\vec{B}_{\parallel} \times \vec{\rho}]\right)\vec{R}_{\perp} + i\frac{\gamma}{2}\vec{K}'_{\perp}\vec{\rho}\right\} \chi_{n_e, n_h}(\vec{\rho} - \vec{\rho}_0), \quad (8)$$

where

$$\gamma = \frac{m_{\perp h} - m_{\perp e}}{M_{\perp}}; \quad \vec{K}'_{\perp} = \vec{K}_{\perp} - \frac{M_{\perp}}{\hbar B_{\parallel}^2} [\vec{B}_{\parallel} \times F_{\perp}];$$

$$\vec{\rho}_0 = \frac{\hbar}{e B_{\parallel}^2} [\vec{B}_{\parallel} \times \vec{K}'_{\perp}]$$

and S is the cross section of the QW, we arrive at the equation for the function χ_{n_e, n_h}

$$\left[-\frac{\hbar^2}{2\mu_{\perp}} \vec{\nabla}^2 + i\frac{e\hbar}{2\mu_{\perp}} \gamma \vec{B}_{\parallel} [\vec{\rho} \times \vec{\nabla}] + \frac{e^2 B_{\parallel}^2}{8\mu_{\perp}} \rho^2 - \frac{e^2}{4\pi\epsilon_0\epsilon} \text{Av} \frac{1}{\sqrt{(\vec{\rho} + \vec{\rho}_0)^2 + (z_e - z_h)^2}} \right] \chi_{n_e, n_h}(\vec{\rho}) = W \chi_{n_e, n_h}(\vec{\rho}). \quad (9)$$

In Eq. (9) $\text{Av}(A) = \langle f_{n_e}(z_e) f_{n_h}(z_h) | A | f_{n_e}(z_e) f_{n_h}(z_h) \rangle$ is the matrix element calculated with respect to the size-quantized functions in Eq. (7). For the total transverse momentum $\vec{K}_{\perp} = K_{\perp} \vec{e}_x$ directed perpendicular to the \vec{e}_z , \vec{e}_y , \vec{B} , \vec{F} plane, the displacement $\vec{\rho}_0$ and the energy W become, respectively,

$$\vec{\rho}_0 = y_0 \vec{e}_y; \quad y_0 = \frac{M_{\perp} \tilde{F}_{\perp}}{e B_{\parallel}^2}; \quad \tilde{F}_{\perp} = F_{\perp} + \frac{\hbar B_{\parallel} K_{\perp}}{M_{\perp}};$$

$$W = E - \frac{\hbar^2 \pi^2}{2d^2} \left(\frac{n_e^2}{m_{\parallel e}} + \frac{n_h^2}{m_{\parallel h}} \right) - \left(1 - \frac{6}{\pi^2} \right) \frac{e^2 B_{\perp}^2 d^2}{24\mu_{\perp}} - \frac{e^2 F_{\parallel}^2 d^4}{\hbar^2} (m_{\parallel e} \delta_{n_e} + m_{\parallel h} \delta_{n_h}) + \frac{\hbar K_{\perp} F_{\perp}}{B_{\parallel}} + \frac{M_{\perp} F_{\perp}^2}{2B_{\parallel}^2}; \quad n_e, n_h = 1, 2, \dots, \quad (10)$$

where

$$\delta_n = -\frac{2^7}{\pi^6} n^2 \sum_{k=1}^{\infty} \frac{(n+2k-1)^2}{(2k-1)^5 (2n+2k-1)^5}; \quad \delta_1 = -\frac{1}{24\pi^2} \left(\frac{15}{\pi^2} - 1 \right) = -2.203 \times 10^{-3}.$$

On the right-hand side of Eq. (10) the third and fourth terms are the shifts of the size-quantized energy level (sec-

ond term) induced by the magnetic B_{\perp} and electric F_{\parallel} (Ref. 13) fields, respectively. It was justified originally in Ref. 14 that the optical absorption can be treated as a transition of the electron-hole pair from the initial state to an excited state having the energy E . These states are described by the wave functions $\Psi_0(\vec{r}_e, \vec{r}_h) = \delta(\vec{r}_e - \vec{r}_h)$ and $\Psi(\vec{r}_e, \vec{r}_h)$ in Eqs. (3), (6), and (8), respectively. The total momentum and the total energy conservation laws lead to the relationships $\vec{K}_{\perp} = \vec{q}$ and $\hbar\omega = E_g + E$, where \vec{q} and ω are the wave vector and frequency of the absorbed photon, respectively. The probability of the transition is determined by the overlap integral of the functions Ψ_0 and Ψ , which in turn provides the selection rules $n_e = n_h \equiv n = 1, 2, \dots$. The coefficient of absorption α can be written in the form¹⁴

$$\alpha = \alpha_0 \sum_E |\chi_{n,\vec{q}}(\vec{\rho}_0)|^2 \delta(\hbar\omega - E_g - E); \quad \alpha_0 = \frac{\pi e^2 |\vec{\eta} \vec{p}_{eh}|^2}{c \epsilon_0 \bar{n} d m_0^2 \omega}. \quad (11)$$

In Eq. (11) $\vec{\eta}$ is the unit polarization vector, \vec{p}_{eh} is the matrix element of the momentum operator, calculated with respect to the Bloch amplitudes of the electron and hole bands, \bar{n} is the refractive index and Σ_E is the sum over the excited states.

III. SPECTRUM OF THE OPTICAL ABSORPTION

A. Fundamental absorption

Here we neglect the electron-hole attraction. In this case the optical absorption is accompanied by the formation of a free electron-hole pair consisting of the electron in the conduction band and a hole in the valence band, respectively. In the absence of the Coulomb interaction the solution to Eq. (9) yields the well-known wave functions $\chi^{(0)}(\vec{\rho})$ and the energies $W^{(0)}$, describing the electron-hole pair in the presence of the magnetic field B_{\parallel} ,¹⁵ given by

$$\chi_{N,m}^{(0)}(\vec{\rho}) = \frac{e^{im\varphi}}{\sqrt{2\pi} a_{B_{\parallel}}} \frac{N!^{1/2}}{(N+|m|)!^{1/2}} s^{(|m|/2)} e^{-(s/2)} L_N^{|m|}(s); \quad s = \frac{\rho^2}{2a_{B_{\parallel}}^2}; \quad (12)$$

$$W_{N,m}^{(0)} = \frac{\hbar e B_{\parallel}}{2\mu_{\perp}} (2N + |m| + \gamma m + 1); \quad N, |m| = 0, 1, 2, \dots, \quad (13)$$

where $L_N^{|m|}(s)$ are associated Laguerre polynomials.¹⁶ Substituting Eqs. (10), (12), and (13) into Eq. (11) we find for the coefficient of the fundamental optical absorption in a narrow QW subject to the tilted parallel magnetic and electric fields

$$\alpha = \alpha_0 \frac{1}{2\pi a_{B_{\parallel}}^2} \sum_{n,N,m} \frac{N!}{(N+|m|)!} s_0^{|m|} e^{-s_0} [L_N^{|m|}(s_0)]^2 \delta(\hbar\omega - E_g - E_{n,N,m}^{(0)}); \quad (14)$$

$$s_0 = \frac{y_0^2}{2a_{B_{\parallel}}^2},$$

where

$$E_{n,N,m}^{(0)} = W_{N,m}^{(0)} + E_{\parallel n} - \frac{\hbar q_{\perp} F_{\perp}}{B_{\parallel}} - \frac{M_{\perp} F_{\perp}^2}{2B_{\parallel}^2}; \quad (15)$$

$$n = 1, 2, \dots; \quad N, |m| = 0, 1, 2, \dots,$$

$$E_{\parallel n} = \frac{\hbar^2 \pi^2 n^2}{2\mu_{\parallel} d^2} + \left(1 - \frac{6}{\pi^2}\right) \frac{e^2 B_{\perp}^2 d^2}{24\mu_{\perp}} + \frac{e^2 F_{\parallel}^2 d^4 M_{\parallel}}{\hbar^2} \delta_n;$$

$$M_{\parallel} = m_{\parallel e} + m_{\parallel h}. \quad (16)$$

B. Exciton absorption

1. Weak magnetic and electric fields ($a_{0\perp} \ll a_{B_{\parallel}}, \tilde{F}_{\perp} \ll \frac{e}{4\pi\epsilon_0\epsilon a_{0\perp}}$)

In this case the wave function $\Psi(\vec{r}_e, \vec{r}_h)$ describes the quasi-2D Coulomb exciton states perturbed by the external fields. It is convenient to take the function (8) in the form

$$\Phi_n(\vec{\rho}_e, \vec{\rho}_h) = \frac{1}{\sqrt{S}} \exp\left\{i\left(K_{\perp} + \frac{e}{2\hbar} [\vec{B}_{\parallel} \times \vec{\rho}]\right) \vec{R}_{\perp}\right\} \chi_n(\vec{\rho}), \quad (17)$$

where χ_n obeys

$$\left[-\frac{\hbar^2}{2\mu_{\perp}} \nabla^2 + i \frac{e\hbar}{2\mu_{\perp}} \gamma \vec{B}_{\parallel} [\vec{\rho} \times \nabla] + \frac{e^2 B_{\parallel}^2}{8\mu_{\perp}} \rho^2 - e\tilde{F}_{\perp} y - \frac{e^2}{4\pi\epsilon_0\epsilon} \text{Av} \frac{1}{\sqrt{\rho^2 + (z_e - z_h)^2}} \right] \chi_n(\vec{\rho}) = \left(W - \frac{M_{\perp} \tilde{F}_{\perp}^2}{2B_{\parallel}^2} \right) \chi_n(\vec{\rho}) \quad (18)$$

and the energy W is given by Eq. (10).

In the zeroth approximation $B_{\parallel} = 0$, $\tilde{F}_{\perp} = 0$, $d = 0$ the solution to Eq. (18) is the 2D exciton states. For the bound states the unperturbed wave functions $\chi^{(0)}$ and the energies $W^{(0)}$ read

$$\chi_{\nu,m}^{(0)}(\vec{\rho}) = \frac{e^{im\varphi}}{\sqrt{2\pi} a_{0\perp}} \frac{4}{p!^{1/2}} \frac{p!^{1/2}}{(p+2|m|)!^{1/2} (2p+2|m|+1)!^{3/2}} u^{|m|} e^{-(u/2)} L_p^{2|m|}(u); \quad u = \frac{2\rho}{a_{0\perp} \nu}, \quad (19)$$

$$W_{\nu}^{(0)} = -\frac{Ry}{\nu^2}; \quad Ry = \frac{\hbar^2}{2\mu_{\perp} a_{0\perp}^2}; \quad \nu = p + |m| + \frac{1}{2}; \quad p, |m| = 0, 1, 2, \dots \quad (20)$$

In a next step of approximation the 2D Coulomb energy levels W become

$$W_\nu(d, B_{\parallel}, \tilde{F}_{\perp}) = W_\nu^{(0)} + \Delta W_\nu(d) + \Delta W_\nu(B_{\parallel}, \tilde{F}_{\perp}) + \frac{M_{\perp} \tilde{F}_{\perp}^2}{2B_{\parallel}^2}, \quad (21)$$

where $\Delta W_\nu(d)$ and $\Delta W_\nu(B_{\parallel}, \tilde{F}_{\perp})$ are the corrections to the 2D Coulomb levels $W_\nu^{(0)}$ caused by the finite width d of the QW and the crossed fields B_{\parallel} and \tilde{F}_{\perp} , respectively. For the ground size-quantized level $n=1$ and for the optically active cylindrically symmetric exciton states, having the magnetic quantum number $m=0$

$$\begin{aligned} \Delta W_\nu(d) &= -\frac{e^2}{4\pi\epsilon_0\epsilon} \langle \chi_{\nu,0}^{(0)}(\vec{\rho}) | \text{Av} \frac{1}{\sqrt{\rho^2 + (z_e - z_h)^2}} - \frac{1}{\rho} | \chi_{\nu,0}^{(0)}(\vec{\rho}) \rangle \\ &= \frac{Ry}{\nu^3} \left(\frac{4}{3} - \frac{5}{\pi^2} \right) \frac{d}{a_{0\perp}}, \\ \nu &= \frac{1}{2}, \frac{3}{2}, \frac{5}{2}, \dots \end{aligned} \quad (22)$$

The effect of crossed magnetic and electric fields on the three-dimensional (3D) Coulomb states has been considered in Refs. 17–19. The nontrivial extension of those results, corresponding to first-order perturbation theory to the 2D exciton states gives

$$\begin{aligned} \Delta W_{\nu,j}(B_{\parallel}, \tilde{F}_{\perp}) &= \sqrt{\left(\frac{3}{2} e \tilde{F}_{\perp} a_{0\perp} \nu \right)^2 + \left(\frac{\hbar e \gamma B_{\parallel}}{2\mu_{\perp}} \right)^2} j; \\ &-\left(\nu - \frac{1}{2} \right) \leq j \leq + \left(\nu - \frac{1}{2} \right). \end{aligned} \quad (23)$$

Since the intensities of the exciton peaks $\sim |\chi_{\nu,0}^{(0)}(0)|^2 \sim \nu^{-3}$ Eq. (19) decrease very rapidly with increasing quantum number ν only the experimentally accessible exciton absorption characteristics, corresponding to the transition to the ground exciton state $\nu=1/2$, will be given below

$$\alpha = \alpha_0 \frac{8}{\pi a_{0\perp}^2} \delta(\hbar\omega - E_g - E_{1/2}), \quad (24)$$

where

$$E_{1/2} = E_{\parallel} + W_{1/2}^{(0)} + \Delta W_{1/2}(d) + \frac{\hbar^2 q_{\perp}^2}{2M_{\perp}} \quad (25)$$

and where the energy $W_{1/2}^{(0)}$ is given by Eq. (20) for $\nu=1/2$. The energy shift $\Delta W_{1/2}(d)$ has been calculated to greater accuracy in Ref. 20

$$\begin{aligned} \Delta W_{1/2}(d) &= 8Ry \left[\left(\frac{4}{3} - \frac{5}{\pi^2} \right) \frac{d}{a_{0\perp}} + \left(\frac{4}{3} - \frac{8}{\pi^2} \right) \right. \\ &\quad \left. \times \left(\frac{d}{a_{0\perp}} \right)^2 \ln \frac{2d}{\pi a_{0\perp}} \right]. \end{aligned} \quad (26)$$

The correction $\Delta W_{1/2}(B_{\parallel}, \tilde{F}_{\perp})$ induced by the crossed fields can then be calculated in second-order perturbation theory that in turn indisputably requires special consideration. This complicated problem relevant to the 3D Coulomb particle has been studied comprehensively by Soloviev.¹⁸

In the vicinity of the first excited exciton peak the satellites caused by the splitting $\Delta W_{\nu,j}$ in Eq. (23) of the exciton level can be observed, in principle. However, the intensities of these peaks are 27 times smaller than that of the ground peak.

2. Strong magnetic fields ($a_{0\perp} \gg a_{B_{\parallel}}$)

In this case the Coulomb interaction can be treated as a small perturbation to the free electron-hole states described by Eqs. (12) and (13). In first-order perturbation theory the energy W in Eq. (9) becomes

$$W_{N,m} = W_{N,m}^{(0)} + \Delta W_{N,m}, \quad (27)$$

where $W_{N,m}^{(0)}$ is the energy of the free electron-hole pair in Eq. (13) and where

$$\Delta W_{N,m} = -\frac{e^2}{4\pi\epsilon_0\epsilon} \langle \chi_{N,m}^{(0)}(\vec{\rho}) | \text{Av} \frac{1}{\sqrt{(\vec{\rho} + \vec{\rho}_0)^2 + (z_e - z_h)^2}} | \chi_{N,m}^{(0)}(\vec{\rho}) \rangle \quad (28)$$

is the correction caused by the electron-hole attraction determined by the matrix element of the Coulomb term in Eq. (9) calculated using the functions $\chi_{N,m}^{(0)}$ in Eq. (12).

In order to simplify the calculations we focus below on the ground state $N=m=0$. Using Eq. (28) we obtain

$$\begin{aligned} \Delta W_{0,0} &= -\sqrt{\frac{\pi}{2}} \frac{e^2}{4\pi\epsilon_0\epsilon a_{B_{\parallel}}} e^{-s_0} \left[e^{s_0/2} I_0\left(\frac{s_0}{2}\right) - \sqrt{\frac{2}{\pi}} \left(\frac{1}{3} - \frac{5}{4\pi^2} \right) \frac{d}{a_{B_{\parallel}}} \right], \end{aligned} \quad (29)$$

where $I_0(x)$ is the modified Bessel function. This result is valid under the condition $y_0 d / a_{B_{\parallel}}^2 \ll 1$. In the limiting case of a weak electric field $\tilde{F}_{\perp}(s_0 \ll 1)$

$$\Delta W_{0,0} = -\sqrt{\frac{\pi}{2}} \frac{e^2}{4\pi\epsilon_0\epsilon a_{B_{\parallel}}} \left[1 - \frac{1}{2} s_0 - \sqrt{\frac{2}{\pi}} \left(\frac{1}{3} - \frac{5}{4\pi^2} \right) \frac{d}{a_{B_{\parallel}}} \right] \quad (30)$$

while for a strong field $\tilde{F}_{\perp}(s_0 \gg 1)$

$$\Delta W_{0,0} = -\frac{e^2}{4\pi\epsilon_0\epsilon |y_0|}. \quad (31)$$

The coefficient of absorption in the vicinity of the ground exciton peak for any s_0 can be calculated from Eq. (14) setting $N=m=0$

$$\alpha = \alpha_0 \frac{1}{2\pi a_{B_{\parallel}}^2} e^{-s_0} \delta(\hbar\omega - E_g - E_{1,0,0} - \Delta W_{0,0}), \quad (32)$$

where $E_{1,0,0}$ is the energy of a free electron-hole pair in Eq. (14) for $n=1$, $N=m=0$ and where $\Delta W_{0,0}$ in Eqs. (29)–(31) is the exciton energy shift.

IV. DISCUSSION

As is well known in bulk material and in the QW of axial symmetry ($\vartheta=0$) the parallel magnetic and electric fields do

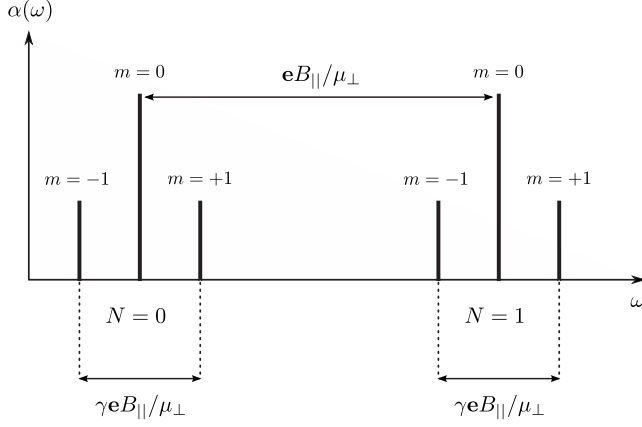


FIG. 2. Sketch of the optical absorption spectrum $\alpha(\omega)$ in Eqs. (14) and (15) caused by the transitions to Landau states with radial quantum numbers $N=0,1$ and magnetic quantum numbers $m=0, \pm 1$.

not lead to an interaction of the motions parallel and perpendicular to the QW axis. The magnetic field governs the states in the plane perpendicular to the fields while the electric field influences only the parallel motion. The resulting total states are superpositions of Landau states and quantum confined Stark states in the QW (Ref. 21) or one-dimensional Franz-Keldysh states in a bulk crystal,^{22,23} which reflect themselves in the corresponding optical absorption spectrum.²⁴ In the QW subject to tilted fields the well potential splits the fields into longitudinal $(\vec{B}_{\parallel}, \vec{F}_{\parallel})$ and transverse $(\vec{B}_{\perp}, \vec{F}_{\perp})$ components with respect to the QW axis. The subsequent induced interaction by the \vec{B}_{\parallel} and \vec{F}_{\perp} on the one hand and \vec{B}_{\perp} and \vec{F}_{\parallel} components on the other hand leads to novel effects demonstrating their interplay. In particular, the interaction induced by \vec{F}_{\perp} and \vec{B}_{\parallel} provides the inversion effect, i.e., the change in the optical peak position $\Delta\omega \sim q_{\perp} F_{\perp} B_{\parallel}^{-1}$ with reversing the direction of the fields \vec{F}_{\perp} or \vec{B}_{\parallel} or the photon wave vector \vec{q}_{\perp} . Also the \vec{F}_{\perp} component generates optical transitions to the axially asymmetric states $m \neq 0$. Along with this the balance between the blue diamagnetic $\sim B_{\perp}^2$ and the red quantum confined Stark $\sim F_{\parallel}^2$ shifts in Eq. (10) does occur.

A. Fundamental absorption

It follows from Eqs. (14) and (15) that the spectrum of the fundamental optical absorption represents a series of Landau N, m peaks in crossed \vec{B}_{\parallel} and \vec{F}_{\perp} fields. Each series is classified with respect to the n th size-quantized subband shifted by the crossed \vec{B}_{\perp} and \vec{F}_{\parallel} fields. Below we concentrate on the experimentally studied main series $n=1$. The qualitative form of the main series $n=1$ of the $N=0,1; m=0, \pm 1$ peaks is given in Fig. 2. The magnetic field \vec{B}_{\perp} induces a diamagnetic blueshift while the electric field \vec{F}_{\parallel} generates a redshift ($\delta_1 < 1$). Under the condition

$$\left(1 - \frac{6}{\pi^2}\right) \frac{B_{\perp}^2}{24\mu_{\perp}} = \frac{F_{\parallel}^2 d^2 M_{\parallel}}{\hbar^2} |\delta_1| \quad (33)$$

these shifts balance each other. The spectrum of the optical absorption with respect to the ground subband $n=1$ coincides

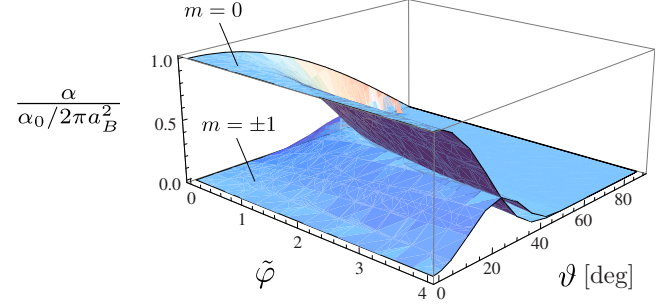


FIG. 3. (Color online) The dependencies of the intensities of the peaks $\alpha_{0,0}$ and $\alpha_{0,\pm 1}$ in Eqs. (14) and (15) for the radial $N=0$ and the magnetic $m=0, \pm 1$ quantum numbers, respectively, scaled to the intensity $\alpha_0/2\pi a_B^2$ ($a_B^2 = \hbar/eB$) on the dimensionless electric field $\tilde{\varphi} = M_{\perp}^2 \tilde{F}_{\perp}^2 / 2\hbar e B^3$ and on the tilted angle ϑ .

with that of a 2D semiconductor given below. It has an effective energy gap E_g^* shifted with respect to E_g toward higher frequencies by an amount corresponding to the ground size-quantized level in the presence of crossed magnetic B_{\parallel} and electric F_{\perp} fields. The peak positions $E_{1,N,m}^{(0)}$ and the gap E_g^* read

$$E_{1,N,m}^{(0)} = E_g^* + \frac{\hbar e B_{\parallel}}{2\mu_{\perp}} (2N + |m| + \gamma m + 1) - \frac{\hbar q_{\perp} F_{\perp}}{B_{\parallel}} - \frac{M_{\perp} F_{\perp}^2}{2B_{\parallel}^2}; \quad N, |m| = 0, 1, 2, \dots$$

and

$$E_g^* = E_g + \frac{\hbar^2 \pi^2}{2\mu_{\parallel} d^2},$$

respectively.

For the weak effective electric field \tilde{F}_{\perp} ($s_0 \ll 1$) the peaks $N=0, 1, 2, \dots; m=0$ are most intense ($\alpha_{N,0} \sim a_B^{-2}$) while the satellite peaks $m \neq 0$ with ($\alpha_{N,m} \sim a_B^{-2} N! (N+|m|)!^{-1} s_0^{|m|}$) are less intense. Measuring in an experiment the frequencies $\Delta\omega$ ($\Delta N=1, m=0$) $= eB_{\parallel}(\mu_{\perp})^{-1}$ between the neighboring $\Delta N=1$ intense peaks $m=0$ and the neighboring $m = \pm 1$ satellites of the N th intense peak $\Delta\omega = eB_{\parallel}(\mu_{\perp})^{-1} \gamma$, depicted in Fig. 2, the electron $m_{\perp e}$ and hole $m_{\perp h}$ transverse effective masses can be determined.

For a strong electric field \tilde{F}_{\perp} ($s_0 \gg 1$)

$$\alpha_{N,m} \sim a_B^2 \frac{1}{N!(N+|m|)!} s_0^{2N+|m|} e^{-s_0}$$

the absorption decreases exponentially with increasing field \tilde{F}_{\perp} . Experimental observation is possible only for electric fields satisfying the condition $s_0 \leq 1$. The dependencies of N, m peaks for $N=0; m=0, \pm 1$ on the electric field \tilde{F} and on the tilted angle ϑ are presented in Fig. 3. The intensity of the main peak $m=0$ monotonically decreases with increasing both the angle ϑ and electric field \tilde{F} while the intensities of the satellites $m = \pm 1$ demonstrate the non-

TABLE I. The band gap E_g , electron m_e and hole m_{hh} masses, dielectric constant ϵ , refractive index n for the GaAs, InGaAs, InGaP, CdZnTe, ZnSe/ZnMnSe (Ref. 25), InAs (Ref. 26), CdTe (Ref. 27), and ZnSe/ZnMgSSe (Ref. 28) QWs. The double balance angle ϑ_0 and corresponding ratio of the electric F and magnetic B fields are calculated from Eqs. (35) and (36), respectively, for the relevant QW width d .

QW	E_g (eV)	m_e/m_0	m_{hh}/m_0	ϵ	n (nm)	d	$\tan \vartheta_0$	ϑ_0°	F/B (10^4 m/s)
GaAs/AlGaAs	1.50	0.067	0.50	12.9	3.6	4.5	0.12	6.9	1.72
InGaAs/InP	0.75	0.044	0.61	13.9	3.6	6.0	0.09	5.2	0.96
InGaP/AlGaInP	1.92	0.13	0.82	11.8	3.6	3.0	0.11	6.3	1.38
CdZnTe/ZnTe	2.07	0.16	1.3	10.1	3.0	2.0	0.08	4.6	1.08
ZnSe/ZnMnSe	2.72	0.14	1.4	8.1	2.7	2.0	0.08	4.6	1.23
InAs/GaAs	0.42	0.023	0.52	15.1	3.5	10.0	0.07	4.0	0.81
CdTe/CdMgTe	1.62	0.096	0.60	10.6	3.5	3.0	0.10	5.7	1.68
ZnSe/ZnMgSSe	2.74	0.15	0.60	9.1	2.9	2.0	0.10	5.7	2.07

monotonic behavior. Equation (15) shows that peak positions can be changed by inverting the directions of the fields \vec{F}, \vec{B} and the wave vector \vec{q}_\perp with the inversion shift $\Delta\omega = 2q_\perp F_\perp B_\parallel^{-1}$.

For the electric field F_\perp satisfying the condition

$$F_\perp + \frac{\hbar B_\parallel q_\perp}{M_\perp} = 0 \quad (34)$$

the parameters $s_0, y_0, \tilde{F}_\perp$ determined by Eqs. (14) and (10) become equal to zero and only the intense peaks $m=0$ remain optically active. If the blue and redshifts [Eq. (33)] and the transverse external and ‘‘centre-of-mass’’ electric fields in Eq. (34) are in balance, respectively, the external electric field F , the centre-of-mass electric field and the transverse magnetic field B_\perp are not manifested. The effects of the B_\perp and F_\parallel on the one hand and of the F_\perp and F_{cm} fields on the other hand are mutually eliminated. It follows from Eqs. (33) and (34) that the corresponding double balance angle ϑ_0 can be calculated from

$$\tan \vartheta_0 = \beta \left(\frac{M_\parallel \mu_\perp}{M_\perp^2} \right)^{1/4} (q_\perp d)^{1/2}; \quad \beta = \left[\frac{24|\delta_1|}{\left(1 - \frac{6}{\pi^2}\right)} \right]^{1/4} = 0.6 \quad (35)$$

and the strengths of the fields should obey the relationship

$$\frac{F}{B} = \beta \frac{\hbar q_\perp^{1/2}}{d^{1/2} (M_\perp^2 M_\parallel \mu_\perp)^{1/4}}. \quad (36)$$

Under the conditions (35) and (36), Eqs. (15) and (16) yield the spectrum of the optical absorption in 2D semiconductor with the energy gap E_g^* in the presence of magnetic field B . This spectrum is formed by equidistant peaks at the positions

$$E_{1,N,0}^{(0)} = E_g^* + \frac{\hbar e B}{2\mu_\perp^*} (2N + 1),$$

where $\mu_\perp^* = \mu_\perp (1 + \tan^2 \vartheta_0)$ is the modified reduced transverse mass. The double balance angle ϑ_0 and corresponding

ratio of the electric F and magnetic B fields are given in Table I. For estimates and simplification of the calculations we take the spherical effective masses $m_{\perp e, hh} \approx m_{\parallel e, hh} \approx m_{e, hh}$. The QWs, possessing a relatively wide energy gap E_g and width d , are favorable for providing the relevant angle ϑ_0 in Eq. (35).

B. Exciton absorption

1. Weak magnetic and electric fields ($a_{0\perp} \ll a_{B\parallel}, \tilde{F}_\perp \ll \frac{e}{4\pi\epsilon_0\epsilon a_{0\perp}^2}$)

For weak magnetic B_\parallel and electric \tilde{F}_\perp fields the optical absorption, corresponding to the transitions to the ground $n=1$ size-quantized state is constituted by a Coulomb series of exciton peaks $\nu=1/2, 3/2, 5/2, \dots$ adjacent from the lower frequencies to the ground size-quantized energy level $E_{\parallel 1}$ in Eq. (16). The intensities of these peaks $\sim |\chi_{\nu,0}^{(0)}|^2$ in Eq. (19) decrease very rapidly $\sim \nu^{-3}$ with increasing quantum number ν . The position of the ground exciton peak $\nu=1/2$ in Eq. (24) is given by the energy $E_{1/2}$ in Eq. (25) consisting of the ground size-quantized energy level $E_{\parallel 1}$ in Eq. (16) shifted toward lower frequencies by an amount $W_{1/2}^{(0)} + \Delta W_{1/2}(d)$ defined by Eqs. (20) and (26), respectively.

Since the binding energy of the exciton E_b is of major interest, we consider below this parameter

$$E_b = E_{n,n,m}^{(0)} - E, \quad (37)$$

where $E_{n,n,m}^{(0)}$ in Eqs. (15) and (16) is the energy of a noninteracting electron-hole pair, and E is the exciton energy, calculated from Eqs. (10) and (18). It follows from Eqs. (10), (15), (16), (18), and (21) that

$$E_{b,1/2}(B, \tilde{F}_\perp, \vartheta) = \frac{\hbar e B_\parallel}{2\mu_\perp} - \frac{M_\perp \tilde{F}_\perp^2}{2B_\parallel^2} - W_{1/2}^{(0)} - \Delta W_{1/2}(d) - \Delta W_{1/2}(B_\parallel, \tilde{F}_\perp), \quad (38)$$

where the energies $W_{1/2}^{(0)}$ and $\Delta W_{1/2}(d)$ are given by Eqs. (20) and (26), respectively, and $\Delta W_{1/2}(B_\parallel, \tilde{F}_\perp)$ is the correction to the ground exciton level caused by the crossed magnetic B_\parallel and electric \tilde{F}_\perp fields. In the case of major differences of the

strengths of these fields this correction induced by only the electric \tilde{F}_\perp (Ref. 29) or exclusively magnetic B_\parallel (Ref. 30) field calculated in second-order perturbation theory is given by the equations

$$\Delta W_{1/2}(B_\parallel, 0) = \frac{3}{32} Ry \left(\frac{a_{0,\perp}}{a_{B_\parallel}} \right)^4;$$

$$\Delta W_{1/2}(0, \tilde{F}_\perp) = -\frac{21}{2^9 Ry} (e\tilde{F}_\perp a_{0,\perp})^2. \quad (39)$$

The effect of comparable fields on the ground 2D exciton state can be equally calculated in second-order perturbation theory by a nontrivial extension of the results obtained for the 3D Coulomb particle.¹⁸ Since the energies $\Delta W_{1/2}(B_\parallel, 0)$ and $\Delta W_{1/2}(0, \tilde{F}_\perp)$ compared to the first and second terms on the right-hand side of Eq. (38), respectively, are on the order of $0.1(a_{0,\perp}/a_{B_\parallel})^2 \ll 1$ and $1/6(a_{0,\perp}/a_{B_\parallel})^4 \ll 1$, respectively, the energy $\Delta W_{1/2}(B_\parallel, \tilde{F}_\perp)$, insignificantly contributes to the binding energy and can be neglected in Eq. (38).

Clearly from Eqs. (26) and (38) we see that with decreasing the width of the QW the exciton binding energy $E_{b,1/2}$ becomes larger. This result is in line with those found both for the impurity in a QW (Ref. 31) and in a QD (Ref. 9) and for the exciton in a QD.¹¹ The dependence of the exciton binding energy in a GaAs/AlGaAs QW on the well width has been calculated numerically in Refs. 32 and 33 providing for the width $d=5$ nm of the light hole exciton $E_{bl}=10.5$ meV (Ref. 32) and $E_{bl}=11.5$ meV (Ref. 33), and for the heavy-hole exciton $E_{bh}=9.6$ meV (Ref. 32) and $E_{bh}=10.3$ meV.³³ These results are close to those obtained from Eq. (38) at $\tilde{F}=B=0$, i.e., $E_{bl}=9.5$ meV and $E_{bh}=11.3$ meV. Note that the discrepancy of our analytical results is of the same order as those calculated in the above-mentioned references. One of the reasons for the difference between our and the numerical data is that the chosen QW for which $d/a_0 \approx (0.3-0.5)$ is not completely in the regime of being a narrow well satisfying the condition $d/a_0 \ll 1$. Also Eq. (38) shows that the binding energy $E_{b,1/2}$ increases with increasing strength of the magnetic field B and for strong values of B the dependence $E_{b,1/2}(B)$ is very close to linear. However, the deviation of the magnetic field from the QW z axis leads to a decrease with respect to the binding energy. The contribution of a tilted magnetic field to the binding energy of the ground exciton state calculated from Eqs. (38) and (39) is shown in Fig. 4. Similar conclusions have been obtained on the base of numerical approaches in Refs. 9, 11, and 31. Reference 31, in which the on-center donor in the CdTe/CdMgTe QW of width $d=10$ nm subject to a tilted weak magnetic field $0 \leq B \leq 16$ T has been considered, is suitable for a more detailed comparison. Setting further in Eq. (38) $\tilde{F}_\perp=0$ and $\mu_\perp \rightarrow m_e$ we obtain from Eqs. (38) and (39)

$$\Lambda_e(B, \vartheta) = \left(\frac{a_e}{a_B} \right)^2 \cos \vartheta \left[1 - \frac{3}{32} \left(\frac{a_e}{a_B} \right)^2 \cos \vartheta \right], \quad (40)$$

where

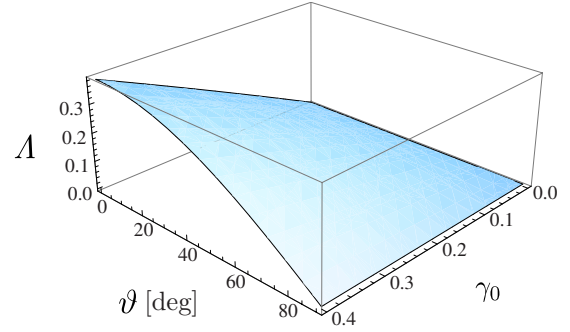


FIG. 4. (Color online) Magnetic shift of the binding energy of the exciton ground state [$\nu=1/2$, Eq. (20)] $E_{b,1/2}(B, \tilde{F}, \vartheta)$ with $\Delta E_{b,1/2} = E_{b,1/2}(B, 0, \vartheta) - E_{b,1/2}(0, 0, \vartheta)$ scaled to the exciton Rydberg constant $\Lambda(B, \vartheta) = \Delta E_{b,1/2} / Ry$ in Eq. (40) as a function of the weak magnetic field B and the tilt angle ϑ . Parameter $\gamma_0 = (a_{0,\perp}/a_B)^2 < 1$ is determined by the exciton Bohr radius $a_{0,\perp}$ and the magnetic length a_B .

$$\Lambda_e(B, \vartheta) = \frac{E_{b,1/2}(B, 0, \vartheta) - E_{b,1/2}(0, 0, \vartheta)}{Ry_e};$$

$$a_e = \frac{4\pi\epsilon_0\epsilon\hbar^2}{m_e e^2}; \quad a_B = \left(\frac{\hbar}{eB} \right)^{1/2}; \quad Ry_e = \frac{\hbar^2}{2m_e a_e^2};$$

In Fig. 5, a comparison of the magnetic shift of the donor binding energy in Eq. (40) with that calculated numerically in Ref. 31 is made for magnetic fields up to 12 T and for the different tilt angles. The analytical dependencies of this shift $E_{b,1/2}(B, 0, \vartheta) - E_{b,1/2}(0, 0, \vartheta)$ on the magnetic field strength and on the tilt angle ϑ are in very good agreement with the corresponding results of variational calculations (Figs. 2 and 3 in Ref. 31), using about 10^3 variational parameters. For larger fields the assumption of a weak magnetic field $a_e \ll a_B$ becomes less appropriate. The critical field B_0 corresponding to the condition $a_e = a_{B_0}$ is about $B_0 \approx 20$ T. The angle shifts of the donor binding energy for weak magnetic fields according to Eq. (40) read

$$\tilde{\Lambda}_e(\vartheta, B) = -2a_e^2 \frac{eB}{\hbar} \sin^2 \frac{\vartheta}{2} \left(1 - \frac{3}{16} a_e^2 \frac{eB}{\hbar} \cos^2 \frac{\vartheta}{2} \right),$$

where

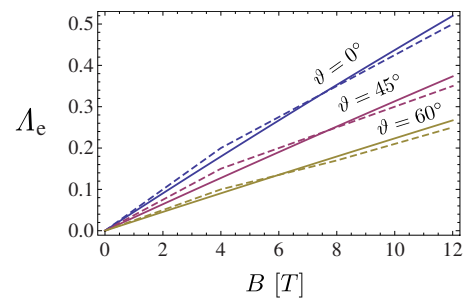


FIG. 5. (Color online) Dimensionless magnetic shift of the donor ground-state binding energy $\Lambda_e(B; \vartheta) = \Delta E_b / Ry_e$ in Eq. (40) versus the magnetic field B for the tilt angles $\vartheta=0^\circ, 45^\circ, 60^\circ$. The dashed lines are the numerical results for the donor in the CdTe/CdMgTe QW ($a_e=5.5$ nm and Ry_e are the donor Bohr radius and the Rydberg constant, respectively) (Ref. 31).

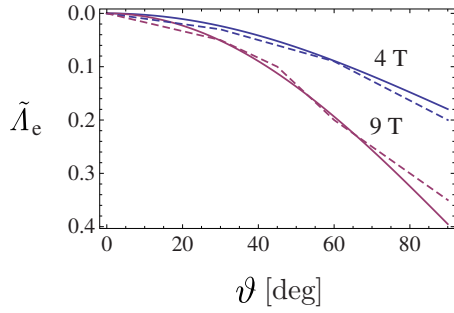


FIG. 6. (Color online) The dependence of the dimensionless angle shift of the donor ground-state binding energy $\tilde{\Lambda}_e(\vartheta; B) = \tilde{\Delta E}_b / Ry_e$, $\tilde{\Delta E}_b = E_b(B, 0, \vartheta) - E_b(B, 0, 0)$ calculated from Eq. (40) on the tilt angle ϑ for the magnetic fields $B=4$ and 9 T. The dashed lines are the numerical results for the donor in a CdTe/CdMgTe QW ($a_e=5.5$ nm and Ry_e are the donor Bohr radius and the Rydberg constant, respectively) (Ref. 31).

$$\tilde{\Lambda}_e(\vartheta, B) = \frac{E_{b,1/2}(\vartheta, 0, B) - E_{b,1/2}(0, 0, B)}{Ry_e}$$

and those extracted from the data of Ref. 31 are compared in Fig. 6. The analytical and numerical results are in good agreement.

Note, that a good agreement between the analytical and variational calculations is obtained in spite of the differences in the structures, i.e., exciton, narrow well of infinite depth in the present work and impurity, well of moderate width and of finite depth in Ref. 31. The reason is that the B and ϑ dependencies of the binding energy are mostly determined by the lateral relative motions of the exciton and impurity, which are nearly identical.

In contrast to the ground exciton state $\nu=1/2$ the excited states $\nu=3/2, 5/2, \dots$ are split by external fields in accordance with Eq. (23). Since the intensities of the first $\nu=3/2$ and second $\nu=5/2$ excited peaks are less than that of the ground $\nu=1/2$ peak by factors of 27 and 125, respectively, the optical transitions to the excited exciton states have not been observed experimentally.

Recently the dependence of the binding energy of the light exciton in a GaAs QD ($m_e=0.067m_0, m_{lh}=0.09m_0$) on a tilted electric field in the presence of a magnetic field directed parallel to the QW z axis has been studied.¹¹ Since the height and the effective radius $R \approx 1.2a_0$ of the QD are of the same order of the exciton Bohr radius $a_0 \approx 17$ nm only a qualitative comparison of the results provided in Ref. 11 and ours, implying the relationship $d \ll a_0$ and a completely unbound ($R \rightarrow \infty$) lateral motion becomes reasonable.

Equation (38) modified such that it is relevant to the parameters employed in Ref. 11 ($B_{\parallel}=B$, $\tilde{F}=F$, $\tilde{F}_{\perp}=F \sin \vartheta$) shows that: (i) the binding energy decreases with increasing strength of the electric field F , (ii) increasing the magnetic field B decreases the effects due to the electric field, and (iii) increasing the tilt angle ϑ the binding energy decreases and the ϑ dependence reduces with the increase in the magnetic field B . All points listed above are in complete agreement with the numerical results [see Fig. 3(b) for (i) and (ii) and

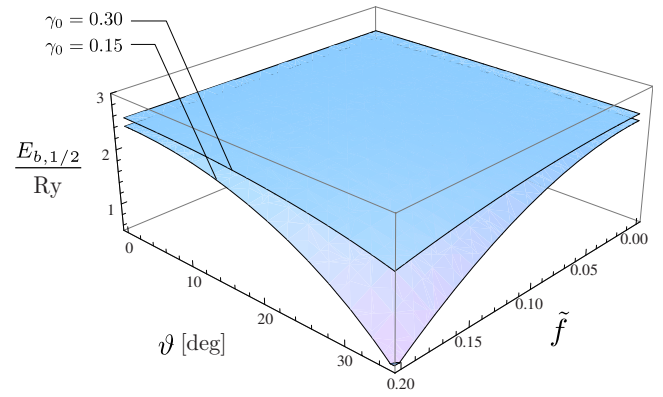


FIG. 7. (Color online) The ground-state exciton binding energy $E_{b,1/2}$ in Eq. (38) scaled with the exciton Rydberg constant Ry as a function of the dimensionless weak electric field $\tilde{f} = e\tilde{F}a_{0\perp}/Ry < 1$ and tilt angle ϑ for weak magnetic fields, determined by the parameter $\gamma_0 = (a_{0\perp}/a_B)^2$. We take $d/a_{0\perp} = 0.4$ and $\mu_{\perp}/M_{\perp} = 0.11$ relevant to the GaAs QW.

Fig. 4 for (iii) in Ref. 11]. Figure 7 shows the binding energy of the exciton subject to weak different magnetic fields in Eq. (38) as a function of the electric field \tilde{F} and the tilt angle ϑ . For the Stark shift of the magnetoexciton energy ΔE_{St} defined in Ref. 11 as $\Delta E_{St} = E(F, B) - E(0, B)$, where the exciton energy E is given by Eqs. (10) and (18) we have for $\vartheta=85^\circ$ $\Delta E_{St} = \Delta W_{1/2}(0, F) < 0$ in Eq. (39). $|\Delta E_{St}|$ parabolically increases with increasing electric field F and does not depend on the magnetic field B . This is in agreement with Fig. 3(c) in Ref. 11. In an effort to perform a qualitative comparison we estimate the effective exciton Rydberg constant \tilde{Ry} from Eq. (38)

$$E_{b,1/2}(B, 0, \vartheta) \approx \frac{\hbar e B}{2\mu_{\perp}} + 4\tilde{Ry}$$

and setting $E_{b,1/2} \approx 20$ meV for $B=1$ T (Ref. 11) we obtain $\tilde{Ry} \approx 4.6$ meV and $\tilde{a}_0 = 15$ nm for the effective exciton Bohr radius. We find for the Stark shift $\Delta E_{St} \approx -2.0$ meV being of the same order of magnitude as $\Delta E_{St} \approx -0.8$ meV from Ref. 11. The discrepancy is due to the difference between the QD and QW. However for the contribution to the exciton binding energy induced by the electric field $\Delta E_{b,1/2}(B, F, \vartheta) = E_{b,1/2}(B, F, \vartheta) - E_{b,1/2}(B, 0, \vartheta)$ we obtain using Eqs. (38) and (39)

$$\Delta E_{b,1/2}(B, F, \vartheta) = -\frac{M_{\perp} F^2}{2B^2} - \Delta W_{1/2}(0, F),$$

i.e., the comparison is favorable. For $B=10$ T, $F=10$ kV/cm and $\vartheta=85^\circ$ we obtain $\Delta E_{b,1/2} = -0.8$ meV, which is in good agreement with the value provided in Ref. 11, Fig. 3(b).

2. Strong magnetic fields ($a_{0\perp} \gg a_{B\parallel}$)

In this case the exciton absorption is in principle the series of fundamental absorption N, m peaks in Eqs. (14) and (15) displaced toward lower frequencies due to Coulomb interaction in Eq. (28). This is given for the ground peak (0,0) in

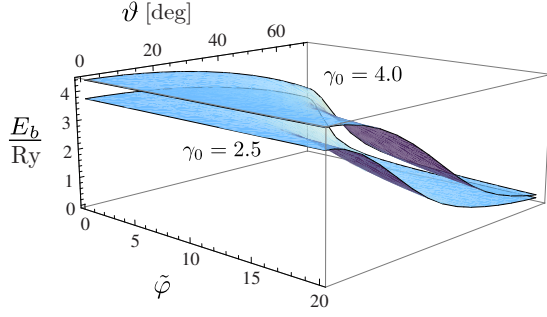


FIG. 8. (Color online) The dimensionless exciton binding energy E_b/Ry (Ry is the exciton Rydberg constant) calculated from Eq. (29) for $E_b = |\Delta W_{0,0}|$ versus the reduced electric field $\tilde{\varphi} = M_{\perp}^2 \tilde{F}^2 / 2\hbar e B^3$ and the tilt angle ϑ . The strong magnetic field B and the width of the QW are $\gamma_0 = (a_{0\perp}/a_B)^2$ and $d/a_{0\perp} = 0.2$, respectively.

explicit form in Eq. (29). It follows that the red exciton shift $\Delta W_{0,0}$ and the exciton binding energy $E_b(B, \tilde{F}, \vartheta) = |\Delta W_{0,0}|$ both decrease with increasing width of the QW, electric field strength \tilde{F} , tilt angle ϑ , and with decreasing the magnetic field strength B . The exciton binding energy versus the electric field \tilde{F} and the tilt angle ϑ in the presence of a strong magnetic field is given in Fig. 8.

The influence of the width of the QW becomes more pronounced with increasing magnetic field B_{\parallel} . For a weak electric field ($s_0 \ll 1$)

$$E_b(B, \tilde{F}, \vartheta) \sim (B \cos \vartheta)^{1/2} \left[1 - a \frac{\tilde{F}^2 \sin^2 \vartheta}{B^3 \cos^3 \vartheta} - b d (B \cos \vartheta)^{1/2} \right],$$

where a and b are positive constants. For a strong electric field ($s_0 \gg 1$)

$$E_b(B, \tilde{F}, \vartheta) \sim \frac{B^2 \cos^2 \vartheta}{\tilde{F} \sin \vartheta}.$$

The contribution of the width of the QW to the exciton energy is negligibly small $\sim \exp(-s_0) \ll 1$ and does not reflect itself in Eq. (31). Thus the dependencies of the exciton binding energy E_b on d , B , F , and ϑ are identical both for weak and strong external fields and possess a universal character. Note that the monotonic increase of the exciton binding energy with decreasing width of the QW up to the value $d \approx 0$ is valid in the approximation of infinite barriers $V_j, j = e, h$, which in turn implies the condition $d > d_j$, where $d_j \approx (\hbar^2 / 2m_j V_j)^{1/2}$. In the region $d < d_j$ the binding energy drastically drops with decreasing width of the QW. For the parameters of a typical GaAs/AlGaAs heterostructure²⁶ $d_e \approx d_{hh} \approx 1.6$ nm, $d_{hh} \approx 0.7$ nm. Thus the approximation of infinite barriers can be applied to GaAs structures studied in Ref. 11 ($d \approx 10$ nm) and in our work ($d \approx 4.5$ nm, see Table I). Moreover our estimates correlate well with the numerical data obtained by Andreani and Pasquarello.³³ They found

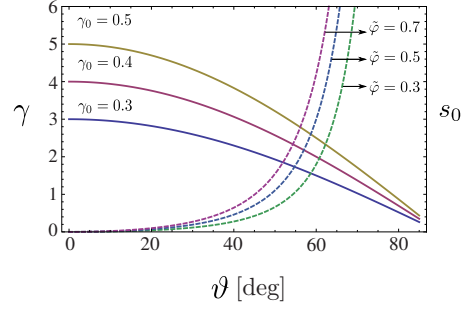


FIG. 9. (Color online) Regimes of strong $\gamma > 1$ ($s_0 > 1$), moderate $\gamma \approx 1$ ($s_0 \approx 1$), and weak $\gamma < 1$ ($s_0 < 1$) magnetic (electric) fields as functions of the tilt angle ϑ with $\gamma = \gamma_0 \cos \vartheta$, $\gamma_0 = (a_{0\perp}/a_B)^2$, $s_0 = \tilde{\varphi} \sin^2 \vartheta \cos^{-3} \vartheta$, $\tilde{\varphi} = M_{\perp}^2 \tilde{F}^2 / 2\hbar e B^3$.

that the exciton binding energy behaves monotonically for QWs wider than 3 nm. The intensities of the exciton peaks exponentially decrease with increasing \tilde{F} and ϑ . However, exciton absorption increases with B . Thus, the exciton absorption remains significant up to external fields satisfying the condition $s_0 \leq 1$ with $s_0 \sim \tilde{F}^2 / B^3$. The conclusions related to the ground (0,0) maximum are qualitatively valid for transitions to other N, m states.

Note that under the condition $F_{\perp} = \hbar B_{\parallel} q_{\perp} / M_{\perp}$ the transverse external electric field F_{\perp} is balanced by the centre of mass electric field $\hbar B_{\parallel} q_{\perp} / M_{\perp}$. In this case $\tilde{F}_{\perp} = 0$ ($y_0 = 0$) and the transverse electron-hole and exciton states are governed only by the longitudinal magnetic field B_{\parallel} . Another important point of the geometry of the tilted fields is the smooth turn from the regime of moderate ($s_0 \approx 1$) to the regimes of weak ($s_0 < 1$) and strong ($s_0 > 1$) electric fields and from the regime of moderate ($a_{0\perp} \approx a_{B\parallel}$) to the regimes of weak ($a_{0\perp} < a_{B\parallel}$) and strong ($a_{0\perp} > a_{B\parallel}$) magnetic fields by keeping the modulus F, B of the external fields constant and changing only the tilt parameter ϑ . The dependence on the parameters γ and s_0 determining the regimes of magnetic and electric fields, respectively, and on the tilt angle is depicted in Fig. 9. In order to estimate the values expected in an experiment, we take typical parameters relevant to the GaAs/AlGaAs material from Table I. In the presence of a magnetic field $B = 20$ T and electric field $F = 50$ kV/cm both tilted at an angle $\vartheta = \pi/4$ the inversion shift $\Delta E = 2\hbar q_{\perp} F_{\perp} / B_{\parallel}$ yields $\Delta E = 8.9$ meV while for the center of mass electric field $F_{\text{cm}} = \hbar B_{\parallel} q_{\perp} / M_{\perp}$ we obtain $F_{\text{cm}} = 0.85$ kV/cm. The balance between the B_{\perp} -blueshift and the F_{\parallel} -redshift of the ground size-quantized electron-hole subband [Eq. (33)] occurs at the fields $F = 40$ kV/cm and $B = 10$ T directed at angle $\pi/4$. An increase of the tilt angle ϑ of the fields $B = 20$ T and $F = 10$ kV/cm from $\vartheta = 20^\circ$ to $\vartheta = 30^\circ$ leads to a considerable decrease of the intensity of the (0,0) peak by a factor of 2.6. For these fields the tilt angles $\vartheta \approx 15^\circ, 30^\circ, 45^\circ$ cover the regimes of a weak ($s_0 \approx 0.24$), moderate ($s_0 \approx 1.25$) and strong ($s_0 \approx 4.5$) electric field F_{\perp} with respect to the magnetic field B_{\parallel} , respectively. In the presence of a magnetic field $B = 20$ T the angles $\vartheta \approx 82^\circ, 70^\circ, 0^\circ$ correspond to a weak ($a_0^2/a_{B\parallel}^2 \approx 0.42$), moderate ($a_0^2/a_{B\parallel}^2 \approx 1$) and strong ($a_0^2/a_{B\parallel}^2 \approx 3$) magnetic field B_{\parallel} . Thus, the typically employed QWs and external tilted fields allow for an experimental

study of novel phenomena associated with the fundamental and exciton absorption in 2D semiconductor structures.

V. CONCLUSIONS

We have developed an analytical approach to the problem of magneto-electroabsorption caused by interband optical transitions specifically to exciton states in a narrow QW subject to parallel tilted external magnetic and electric fields. The dependencies of the coefficient of the fundamental and exciton absorption on the strengths of the external fields, width of the QW, exciton parameters and the tilt angle have been obtained in an explicit form. The center of mass electric field caused by the motion of the center of mass of the electron-hole pair in the magnetic field is taken into account. Novel effects unique for the QW and tilted parallel fields are found to occur. The interaction induced by the center of mass and external electric fields leads to an inversion effect. The optical absorption changes with reversing the direction of one of the external fields or the wave vector of the photon. Under specific conditions the blue diamagnetic and red quantum confined Stark shifts of the peak position balance each other. Equally the center of mass and external electric fields can cancel each other. Being directed at the double balance tilt angle characterizing the concrete QW the external fields satisfy both conditions. In this case some of effects induced by these fields become balanced that in turn simplifies the form of the optical spectrum. A weak tilted electric field provides optical absorption maxima forbidden in the absence of this field. Sufficiently strong tilted electric fields lead to an

exponential decrease of the absorption with increasing electric field strength. With increasing magnetic field the optical absorption increases. In the presence of weak magnetic and electric fields the Coulomb electron-hole interaction provides Rydberg series of exciton peaks located below the size-quantized levels slightly modified by the external fields. For strong magnetic fields the exciton effect leads to a redshift of the peak positions associated with the fundamental absorption. The exciton binding energy increases with increasing magnetic field strength and narrower QW while it decreases with increasing electric field strength as well as tilt angle. The influence of the width of the QW becomes more pronounced for stronger magnetic fields. The geometry of the tilted fields allows to turn smoothly from the regimes of moderate to the regimes of weak and strong fields by keeping the strengths of the fields and changing only the tilt angle. Note that the absolute majority of the observed effects are not present in bulk material and in a QW subject to external fields both directed parallel to the QW axis. Estimates of the expected values calculated for the typically employed GaAs/AlGaAs QWs, strengths of external fields and tilt angles show that the above-mentioned phenomena can be observed experimentally.

ACKNOWLEDGMENTS

The authors are grateful to V. Aguekian for valuable discussions, and B. Chatterjee and C. Morfonios for technical assistance. Financial support by the Deutsche Forschungsgemeinschaft is gratefully acknowledged.

*Permanent address: Department of Physics, State Marine Technical University, 3 Lotsmanskaya Str., 190008 St. Petersburg, Russia.

¹J. C. Maan, in *Two Dimensional Systems, Heterostructures, and Superlattices*, edited by G. Bauer, F. Kuchar, and H. Heinrich (Springer-Verlag, Berlin, 1984), p. 183.

²R. Merlin, *Solid State Commun.* **64**, 99 (1987).

³G. Yu, D. J. Lockwood, A. J. Spring Thorpe, and D. G. Austing, *Phys. Rev. B* **76**, 085331 (2007).

⁴S. Takaoka, A. Kuriyama, K. Oto, K. Murase, S. Shimomura, S. Hiyamizu, M. Cukr, T. Jungwirth, and L. Smrcka, *Physica E* **6**, 623 (2000).

⁵T. M. Fromhold, A. A. Krokhin, C. R. Tench, S. Bujkiewicz, P. B. Wilkinson, F. W. Sheard, and L. Eaves, *Phys. Rev. Lett.* **87**, 046803 (2001).

⁶L. V. Butov, A. A. Shashkin, V. T. Dolgoplov, K. L. Campman, and A. C. Gossard, *Phys. Rev. B* **60**, 8753 (1999).

⁷M. de Dios-Leyva, C. A. Duque, and L. E. Oliveira, *Phys. Rev. B* **76**, 075303 (2007).

⁸A. L. Morales, N. Raigoza, C. A. Duque, and L. E. Oliveira, *Phys. Rev. B* **77**, 113309 (2008).

⁹F. J. Ribeiro, A. Latge, M. Pacheco, and Z. Barticevic, *J. Appl. Phys.* **82**, 270 (1997).

¹⁰M. Sugisaki, H. W. Ren, S. V. Nair, K. Nishi, and Y. Masumoto, *Phys. Rev. B* **66**, 235309 (2002).

¹¹D. Wang, G. Jin, Y. Zhang, and Y. Ma, *J. Appl. Phys.* **105**, 063716 (2009).

¹²R. Lamb, *Phys. Rev.* **85**, 259 (1952).

¹³F. M. Fernandez and E. A. Castro, *Physica A* **11A**, 334 (1982).

¹⁴R. J. Elliott, *Phys. Rev.* **108**, 1384 (1957).

¹⁵L. P. Gor'kov and I. E. Dzyaloshinskii, *Sov. Phys. JETP* **26**, 449 (1967).

¹⁶*Handbook of Mathematical Functions*, edited by M. Abramowitz and I. A. Stegun (Dover, New York, 1972).

¹⁷Yu. N. Demkov, B. S. Monozon, and V. N. Ostrovskii, *Sov. Phys. JETP* **30**, 775 (1970).

¹⁸E. A. Solov'ev, *Sov. Phys. JETP* **58**, 63 (1983).

¹⁹P. A. Braun and E. A. Solov'ev, *Sov. Phys. JETP* **59**, 38 (1984).

²⁰B. S. Monozon and P. Schmelcher, *Superlattices Microstruct.* **26**, 229 (1999).

²¹D. A. B. Miller, D. S. Chemla, T. C. Damen, A. C. Gossard, W. Wiegmann, T. H. Wood, and C. A. Burrus, *Phys. Rev. Lett.* **53**, 2173 (1984).

²²B. S. Monozon and M. V. Pevzner, *Sov. Phys. Semicond.* **4**, 390 (1970).

²³T. G. Pedersen and T. B. Lyngø, *Phys. Rev. B* **65**, 085201 (2002).

²⁴S. Benner and H. Haug, *Phys. Rev. B* **47**, 15750 (1993).

²⁵M. Sugawara, *J. Appl. Phys.* **71**, 277 (1992).

²⁶E. H. Li, *Physica E* **5**, 215 (2000).

- ²⁷P. Harrison, *Quantum Wells, Wires and Dots* (Wiley, New York, 2000).
- ²⁸T. Miyajima, F. P. Loque, J. F. Donegan, and J. Hegarty, *Appl. Phys. Lett.* **66**, 180 (1995).
- ²⁹K. Tanaka, M. Kobashi, T. Shichiri, T. Yamabe, D. M. Silver, and H. J. Silverstone, *Phys. Rev. B* **35**, 2513 (1987).
- ³⁰O. Akimoto and H. Hasegawa, *J. Phys. Soc. Jpn.* **22**, 181 (1967).
- ³¹P. Redliński and B. Janko, *Phys. Rev. B* **71**, 113309 (2005).
- ³²G. E. W. Bauer and T. Ando, *Phys. Rev. B* **38**, 6015 (1988).
- ³³L. C. Andreani and A. Pasquarello, *Phys. Rev. B* **42**, 8928 (1990).